Direct Observation of Self-Similarity in Evolution of Transient Stimulated Raman Scattering in Gas-Filled Photonic Crystal Fibers

A. Nazarkin, A. Abdolvand, A. V. Chugreev, and P. St.J. Russell

*Max-Planck Institute for the Science of Light, Guenther-Scharowsky Strasse 1/24, 91058 Erlangen, Germany**

(Received 6 July 2010; published 20 October 2010)

A unique characteristic of transient stimulated Raman scattering, in which the spatiotemporal evolution of the fields and the molecular excitation follow a universal self-similarity law, is observed in gas-filled photonic crystal fibers. As the input laser power is increased, the coupled system ''optical fields + molecular excitation'' goes through the same phases of time evolution but at a higher rate. Using the self-similarity law we are able to completely reconstruct the evolution of the pump and Stokes fields from one measurement.

DOI: 10.1103/PhysRevLett.105.173902 PACS numbers: 42.70.Qs, 42.50.Md, 42.65.Dr, 42.65.Tg

Resonant laser-matter interactions, in regimes where the pulse duration is shorter than the phase relaxation time T_2 of an atomic or molecular transition (coherent interaction), are of great theoretical and experimental interest. This is motivated by the importance of coherent optical phenomena in ultrafast spectroscopy, short pulse frequency conversion, and studies of nonlinear dynamics in complex systems [1]. While coherent phenomena exhibit quite diverse nonlinear behavior, it has been found that fundamental processes such as pulse propagation in coherent absorbers and amplifiers, superradiant decay, and transient stimulated Raman scattering (SRS) can be treated in a universal way. This appears to be possible because under certain conditions the Maxwell-Bloch equations describing these processes are integrable and, in particular, can be reduced to the sine-Gordon equation (SGE) for the evolution of Bloch spins [1]. Solitonic solutions of the SGE are associated with 2π pulses in self-induced transparency, processes which have been observed and studied experimentally in great detail [2,3]. In contrast, markedly different behavior is predicted for nonsolitonic solutions of the SGE, which are associated with coherent pulse amplification [4,5], superradiant decay [1,6], and transient stimulated Raman scattering [7,8]. A fundamental hypothesis is that at long interaction lengths the spatiotemporal evolution of these nonsolitonic solutions should be self-similar; i.e., at each point in the medium the system should go through the same phases of temporal evolution but within a different time. This occurs only if the laser-matter interaction is coherent. Although some features of the predicted dynamics have been observed before (i.e., π-pulse shortening in laser amplifiers [9,10] and time modulation of the fields in SRS [11,12]), so far no clear signature of self-similarity of this process has been established.

In this Letter we report for the first time the observation of clear self-similar behavior in transient stimulated Raman scattering by carrying out a detailed study of transient SRS over long interaction lengths. To do this we make use of the unique characteristics of gas-filled hollow-core photonic crystal fiber (HC PCF) [13,14]. These novel optical guiding systems offer interaction lengths many times longer than the Rayleigh length of a focused laser beam, while eliminating diffraction by keeping the beam tightly confined in a single mode. Moreover, by designing a HC PCF with restricted bandwidth of guidance, the Raman process can be completely isolated from competing higher-order SRS processes. In this way, we are able to make detailed measurements of (and gain insight into) late-stage transient SRS when quantum conversion to the Stokes is close to unity.

The relationship between SRS and the SGE can be established by considering the transient limit of the semiclassical equations of SRS [7,8,12]. Consider pump and Stokes waves propagating in a Raman medium in the $+z$ direction and represented by $E_{p,s}(z,t) = A_{p,s}(z,t) \times \exp(i\omega_{p,s}t - ik_{p,s}z) + \text{c.c}$, where $A_{p,s}$ are the complex electric field amplitudes, $k_{p,s} = k(\omega_{p,s})$ are the field propagation constants, and $\omega_{p,s}$ the carrier frequencies of the fields, which are resonant with the Raman transition frequency, i.e., $\Omega = \omega_p - \omega_s$. In the regime of weak excitation of the Raman transition ($n \approx n_0 = 1$), the interaction dynamics is described by the equation for the off-diagonal density-matrix element ρ_{12}, while the spatiotemporal evolution of the fields obeys the wave equations

$$\frac{\partial \rho_{12}}{\partial \tau} = i\frac{r_{12}}{4\hbar}A_p A_s^* - \frac{\rho_{12}}{T_2}, \qquad \frac{\partial A_p}{\partial \zeta} = i\kappa\rho_{12}A_s,$$
$$\frac{\partial A_s}{\partial \zeta} = i\kappa^{-1}\rho_{12}^* A_p, \tag{1}$$

where $\tau = t - z/v$ is the retarded time (v is the group velocity, assumed to be equal for both pulses). The dimensionless distance ζ is introduced by normalizing z to $L_{\text{SRS}} = c/2\pi N r_{12}\sqrt{\omega_p\omega_s/n_p n_s}$, where N is the number density of molecules, $\kappa = \sqrt{\omega_p n_s/\omega_s n_p}$, and r_{12} is the matrix element characterizing the coupling of the fields to the Raman transition. It is assumed that the fields have

finite energy, so that no permanent solitonlike structures can exist in the system [8]. Below we consider a special solution of Eqs. (1) where the fields are taken as real-valued quantities and the coherence of the Raman transition is purely imaginary, i.e., $\rho_{12} = i\rho$, $\mathrm{Im}(\rho) = 0$. These special solutions are most significant from a physical viewpoint because they correspond to the case of maximum Raman gain. Conservation of photon number allows one to rewrite the field amplitudes formally using the new variable $\psi(\zeta, \tau)$:

$$A_p(\zeta, \tau) = \kappa^{1/2} A_0(\tau) \cos(\psi/2),$$
$$A_s(\zeta, \tau) = \kappa^{-1/2} A_0(\tau) \sin(\psi/2), \quad (2)$$

where $A_0^2(\tau) = \kappa^{-1} A_p^2(\tau) + \kappa A_s^2(\tau)$, and $A_p(\tau)$ and $A_s(\tau)$ are the temporal shapes of the fields at the medium input $\zeta = 0$. By inserting representation (2) into Eqs. (1), and assuming the transient interaction regime ($\tau_p \ll T_2$), the three equations in (1) are reduced to only one equation for the function $\psi(\zeta, \tau)$:

$$\frac{\partial^2 \psi}{\partial \zeta \partial \tau} = \frac{r_{12}}{4\hbar} A_0^2(\tau) \sin\psi. \quad (3)$$

After introducing a new time variable $T(\tau) = \frac{r_{12}}{4\hbar} \times \int_{-\infty}^{\tau} A_0^2(\tau') d\tau'$, one arrives at the SGE:

$$\frac{\partial^2 \psi}{\partial \zeta \partial T} - \sin\psi = 0. \quad (4)$$

Below we consider self-similar solutions $\tilde{\psi}(\chi)$ of Eq. (4), which depend only on the variable $\chi = 2\sqrt{\zeta T}$. These solutions obey the following equation:

$$\frac{\partial^2 \tilde{\psi}}{\partial \chi^2} + \frac{1}{\chi} \frac{\partial \tilde{\psi}}{\partial \chi} - \sin\tilde{\psi} = 0. \quad (5)$$

Physically interesting solutions of Eq. (5) are defined by the boundary conditions at $\chi = 0$, $\tilde{\psi}(0) = \tilde{\psi}_0$ and $\tilde{\psi}'(0) = 0$, which suggest that before the fields arrive there is no excitation of the Raman medium [7,8]. The universal function $\tilde{\psi}(\chi)$ describes all the system dynamics and does not depend on the form of the fields. The region $0 < \chi < 1$ corresponds to early-stage Stokes generation when $\tilde{\psi}(\chi) \propto I_0(\chi)$ [$I_0(x)$ is a Bessel function of the second kind] and the Stokes field has a smooth temporal profile. For $\chi \gg 1$ (late stage), $\tilde{\psi}(\chi)$ oscillates with decreasing amplitude, asymptotically approaching π, which corresponds to complete conversion of photons to the Stokes field.

To observe the self-similar behavior predicted by Eqs. (2) and (5), we carried out SRS experiments in gas-filled HC PCF (see Fig. 1). We used a narrow linewidth laser delivering 10 ns pulses of a 100 μJ energy at $\lambda_p = 1.064$ μm. The pump pulses were launched into a photonic

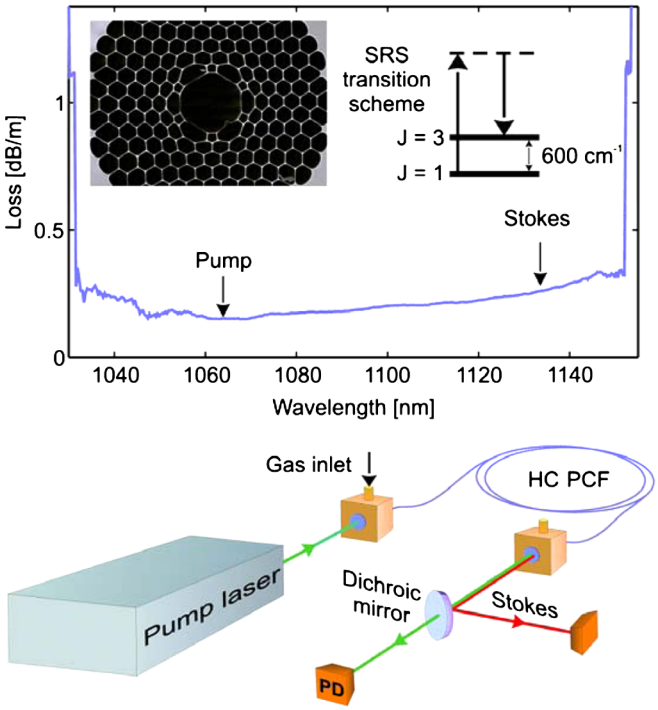

FIG. 1 (color online). Nanosecond laser pulses are launched into a low-loss band-gap HC PCF filled with hydrogen, exciting the rotational transition $J = 1$ to $J = 3$. The narrow transmission band of the fiber allows only the pump and Stokes fields to propagate in the gas-filled core. The inset shows a scanning electron micrograph of the HC-PCF microstructure.

band gap HC PCF (core size $D = 12$ μm) filled with hydrogen. The PCF had a low-loss transmission window between 1030 and 1150 nm, which meant that only the pump and first Stokes bands, interacting with the $J = 1$ to $J = 3$ rotational transition (frequency shift 600 cm^{-1}) could propagate in the fiber [14]. As a result, the competing vibrational and higher-order rotational SRS typically present in a focused beam geometry were completely suppressed. The gain line of forward SRS in hydrogen is predominantly collision broadened (for H_2 the value is 50 MHz/bar [14]). Note that inhomogeneous (Doppler) broadening is important at pressures much lower than the working pressures we used ($p = 1, \ldots, 2$ bar). In this pressure region the Raman line is additionally broadened by 200 MHz through collisions with the core sidewalls, resulting in a net phase relaxation time $T_2 = 5$ ns at 1 bar.

The length of the HC PCF was $L = 200$ cm. At $p = 1$ bar the effective Raman length was $L_{\mathrm{SRS}} = 0.1$ cm, and the gain G was as high as 0.15 cm^{-1} for pump energies of $\sim$20 μJ, bringing GL up to a value of 30, the threshold for SRS. As a result, we were able to operate in a regime where quantum conversion to the Stokes was close to 100%. For the 10 ns pump pulses with $I_p \sim 1$ GW/cm^2, spectral broadening due to self-phase modulation (SPM) in H_2 was negligibly small (the estimated nonlinear phase shift $\delta\varphi_{\mathrm{SPM}} < 10^{-5}$). Although the pump pulse duration was

somewhat greater than T_2, the transient dynamics were very clear. This is explained by the sharply increasing SRS gain at the front of the pump pulse, leading to a Stokes field rise time much less than T_2.

Experimental plots of the temporal structure of the pump and Stokes pulses (averaged over 500 shots) for different values of pump pulse energy are given in Fig. 2. For relatively low pump energies ($< 30\ \mu$J) the pulse shapes are quite smooth. At higher input pump energies, however, well-pronounced oscillations appear, with a period that shortens as the pump energy increases. The time scale of these oscillations (or "ringing") is ~ 1 ns, which is shorter than $T_2 = 5$ ns, suggesting that the Raman scattering is strongly coherent and the nonlinear interaction is late-stage. Their origin can be explained as follows. The growth of the Stokes field leads to significant pump depletion, while the molecular coherence ρ_{12} still remains nonzero due to the presence of "coherent memory." As a result, a new field at the pump frequency is generated at the expense of the Stokes field. Because the phase of this new field is shifted by π, the coherence goes through zero and changes its sign. This leads to oscillating field dynamics and molecular response.

The most interesting fact established by our study is that the output pulse shapes are self-similar. To demonstrate this, we now express the field intensities as functions of $\psi(\zeta, \tau)$, which is supposed to behave in a self-similar way. Because Stokes generation starts from a very small (spontaneous) signal, at the input we have $A_s^2(\tau) \ll A_p^2(\tau)$, leading from Eq. (2) to $A_0^2(\tau) \approx \sqrt{\omega_s n_p/\omega_p n_s} A_p^2(\tau)$. Considering now data sets resulting from dividing the intensity distributions of the output pump $I_P(\zeta = \zeta_L, \tau)$ and Stokes $I_P(\zeta = \zeta_L, \tau)$ pulses by the input pump pulse shape $I_P(\zeta = 0, \tau) = I_{P0}(\tau)$ (where $\zeta_L = L/L_{\mathrm{SRS}}$ is the normalized fiber length), we can write

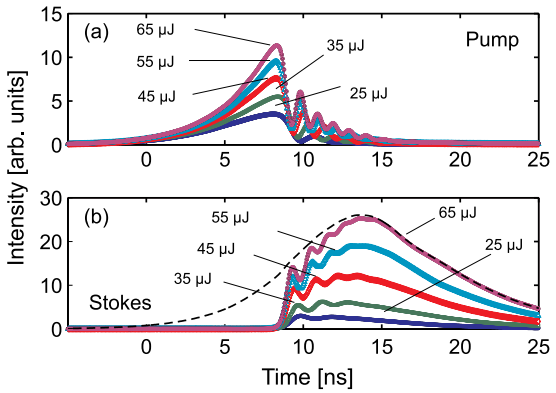

FIG. 2 (color online). Measured output pump (a) and Stokes (b) pulse shapes (each one is averaged over 500 shots) for input pump energies from 25 to 65 μJ. All input pump pulses have the same Gaussian form with FWHM duration 10 ns (an input pump pulse of a 65 μJ energy is shown with a dashed line in (b).

$$\frac{I_P^{(i)}(L,\tau)}{I_{P0}^{(i)}(\tau)} = \cos^2\frac{\psi^{(i)}}{2}, \qquad \frac{I_S^{(i)}(L,\tau)}{I_{P0}^{(i)}(\tau)} = \frac{\omega_S}{\omega_P}\sin^2\frac{\psi^{(i)}}{2}, \quad (6)$$

where $i = 1, 2, \ldots, n$ labels the output pump and Stokes intensities in Fig. 2 corresponding to the ith input pump pulse intensity $I_{P0}^{(i)}(\tau)$. If the behavior of the measured output intensity distributions are self-similar, then the ratios on the left-hand sides of Eqs. (6) should depend, through the functions $\psi^{(i)}(L,\tau) = \tilde{\psi}(\chi^{(i)})$, only on the self-similarity variable:

$$\chi^{(i)} = 2\sqrt{LT_{(i)}} = 2\sqrt{\beta L I_0^{(i)} \int_{-\infty}^{\tau} f_p(\tau')d\tau'}, \quad (7)$$

where we have introduced the form factor $f_P(\tau) = I_{P0}^{(i)}(\tau)/I_0^{(i)}$ for the input pulses, $I_0^{(i)}$ being the peak intensity of the ith pulse and $\beta = 2\pi|r_{12}|/(n_p c\hbar)$. Equation (7) suggests that changing the input pulse energy will simply alter the range of variation of $T_{(i)}$ and $\chi^{(i)}$. As a result the ratios $I_P^{(i)}(L,\tau)/I_{P0}^{(i)}(\tau)$ and $I_S^{(i)}(L,\tau)/I_{P0}^{(i)}(\tau)$, when plotted as a function of $T_{(i)}$ (proportional to the integrated input pump intensity), should exhibit the same (universal) behavior for every input pump pulse. In Fig. 3 we plot the ratios in Eqs. (6) as a function of $T_{(i)}$ for pump energies of 35, 45, 55, and 65 μJ. The curves almost completely agree (within experimental error), suggesting that the late-stage dynamics of the SRS process are indeed self-similar. The somewhat smaller modulation depth for 35 μJ can be explained by the fact that a weaker pump pulse generates slower temporal modulations (see Fig. 2), which are more strongly affected by the relaxation process. The behavior in Fig. 3 is associated with the functions $\sin^2(\tilde{\psi}/2)$ and

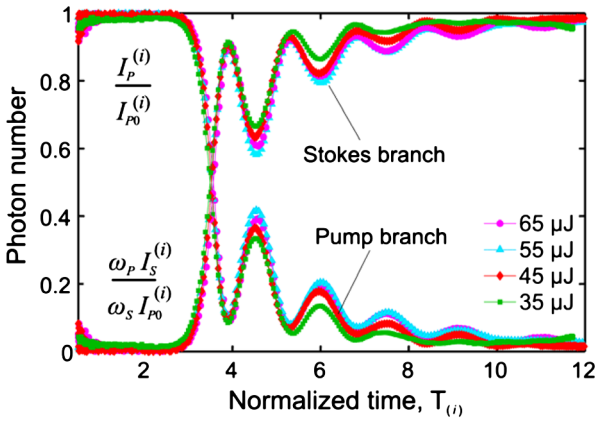

FIG. 3 (color online). Dependence of the ratios $I_P^{(i)}/I_{P0}^{(i)}$ and $I_S^{(i)}/I_{P0}^{(i)}$ on the integrated intensity $T_{(i)}$ of the input pump pulse for different pump energies (35, 45, 55, and 65 μJ), indicating the behavior of squared sine and cosine functions of the universal self-similarity function $\tilde{\psi}$. The damped oscillations of the ratios clearly show the underlying self-similar oscillatory behavior of the system for different power levels.

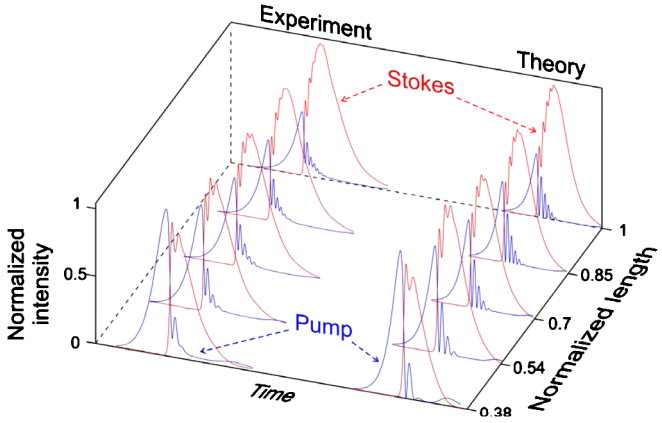

FIG. 4 (color online). Reconstruction of pump and Stokes pulse shapes for a launched pulse energy of 65 μJ. Experiment: Snapshots of the pulse shapes at different positions along the fiber, obtained using the equivalence of length and pulse energy (see text). Theory: Pulse shapes (input pump energy 65 μJ) calculated with the exact model in Eqs. (1).

$\cos^2(\tilde{\psi}/2)$, where the universal function $\tilde{\psi}$ completely characterizes the evolution of the system. As we have already established, this function is independent of the shape of the input pulse and depends only on the parameters of the Raman medium.

Since the similarity variable depends on the product of L and $I_0^{(i)}$, increasing the input pulse energy will have the same effect as lengthening the fiber, allowing us to reconstruct from our data the pump and Stokes pulse shapes at different positions along the fiber. For example, the pulse shapes at position $L/2$ for a launched pulse of energy of 65 μJ will be identical to those at L for a pulse energy of 32.5 μJ. Applying this procedure to the data in Fig. 2, we were able to reconstruct the pulse shapes at several positions along the fiber for a launched energy of 65 μJ. The results are shown in Fig. 4. We also present the results of numerical modeling of SRS inside the fiber based on solutions of the exact equations, assuming input parameters (pulse energy and shape, gas pressure, phase relaxation time) close to the experimental values. Good agreement is obtained between theory and the experimental data, confirming the self-similar character of the transient SRS process. From these results it follows that just one measurement of output pump and Stokes pulse shapes is sufficient to extract the form of the universal function and predict the system evolution for different input conditions. Full reconstruction is possible because these self-similar solutions belong to a class of exact solutions of the SGE in which no information is lost.

In fact, the experimental result presented here for the first time extend the field of self-similarity [15] to the broad class of nonlinear systems described by the SGE.

One further interesting consequence of self-similarity is that it clarifies the behavior of the pump and Stokes fields during the initial stages of spontaneous Raman scattering in the transient regime, when the Stokes intensity increases linearly with distance; the semiclassical equations normally used to describe SRS do not treat this regime. Self-similarity delivers an unambiguous answer to this question. From the solutions for the fields in Eq. (2) and the boundary conditions at $\zeta \to 0$ for the self-similarity function $\tilde{\psi}$, we find that $A_s(\tau)/A_p(\tau) = \text{const}$. This means that, if self-similar behavior is to be observed, the input temporal shape of the Stokes pulse must exactly reproduce the temporal shape of the pump pulse. Therefore, the observed behavior is a manifestation of an important prediction of quantum theory [16], namely, that at the spontaneous stage of transient Raman scattering the statistically averaged Stokes intensity and spectrum of transient Raman process should follow the intensity and spectrum of the pump pulse.

*www.pcfibre.com

[1] L. Allen and J. H. Eberly, *Optical Resonance and Two-Level Atoms* (Wiley, New York., 1975).
[2] S. L. McCall and E. L. Hahn, Phys. Rev. **183**, 457 (1969).
[3] G. L. Lamb, Rev. Mod. Phys. **43**, 99 (1971).
[4] F. A. Hopf and M. O. Scully, Phys. Rev. **179**, 399 (1969).
[5] S. V. Manakov, Sov. Phys. JETP **56**, 37 (1982).
[6] I. P. Gabitov, V. E. Zakharov, and A. V. Mikhailov, Sov. Phys. JETP **59**, 703 (1984).
[7] J. N. Elgin and T. B. O'Hare, J. Phys. B **12**, 159 (1979).
[8] C. R. Menyuk *et al.*, Phys. Rev. Lett. **69**, 3048 (1992); Phys. Rev. A **47**, 2235 (1993).
[9] O. P. Varnavskii *et al.*, Sov. Phys. JETP **59**, 716 (1984).
[10] J. D. Harvey *et al.*, Phys. Rev. A **40**, 4789 (1989).
[11] M. D. Duncan *et al.*, J. Opt. Soc. Am. B **5**, 37 (1988).
[12] R. L. Carman *et al.*, Phys. Rev. A **2**, 60 (1970).
[13] P. St. J. Russell, J. Lightwave Technol. **24**, 4729 (2006).
[14] A. Abdolvand, A. Nazarkin, A. V. Chugreev, and P. St. J. Russell, Phys. Rev. Lett. **103**, 183902 (2009).
[15] G. I. Barenblatt, *Scaling, Self-Similarity, and Intermediate Asymptotics* (Cambridge University Press, Cambridge, England, 1996).
[16] M. G. Raymer and J. Mostowski, Phys. Rev. A **24**, 1980 (1981); M. D. Duncan *et al.*, J. Opt. Soc. Am. B **8**, 300 (1991).